

*Form of opening (renewal) for Project*

APPROVED

JINR DIRECTOR

\_\_\_\_\_  
/\_\_\_\_\_  
" " \_\_\_\_\_ 2025

**SCIENTIFIC AND TECHNICAL REASONING FOR THE OPENING / RENEWAL  
OF THE PROJECT IN RESEARCH AREA  
WITHIN THE TOPICAL PLAN FOR JINR RESEARCH**

**1. General information on the project**

**1.1. Theme code** (for renewable project / subproject) - *the theme code includes the opening date, the closing date is not given, as it is determined by the completion dates of the projects in the topic.*

02-2-1151-1-2025 Development of advanced detectors and analysis methods, hadronic and rare leptonic processes

**1.2. Project** (for renewed project)

02-2-1151-2-2026/2027

**1.3. Laboratory**

Dzhelepov Laboratory of Nuclear Problems

**1.4. Scientific field**

Elementary Particle Physics and High-Energy Heavy-Ion Physics (02)

**1.5. The name of the Project**

Development of a physics program and detectors for experiments at CEPC

**1.6. Project Leader(s)**

Yuri Davydov  
Alexey Zhemchugov

**1.7. Project Deputy Leader(s)**

Yuri Kulchitsky  
Andrej Arbuzov

**1.8. Scientific supervisor of the project**

## 2. Scientific rationale and organisational structure

### 2.1. Annotation

The discovery of the Higgs boson at the LHC marked the beginning of a new era in high-energy physics. Precision measurements of the properties of the Higgs boson and the exploration of new physics beyond the Standard Model (BSM) using the Higgs boson as an instrument seem to be a natural next step after the LHC and High Luminosity LHC (HL-LHC). Most attractive for this are electron-positron colliders, several projects of which – ILC, CLIC, and FCC-ee – have been put forward in the last two decades. In 2012, a circular electron-positron collider (CEPC) project with a circumference of 100 km was proposed in China. CEPC is an  $e^+e^-$  Higgs factory for the production of Higgs/W/Z bosons, which is designed for unprecedentedly accurate Higgs measurements, verifying predictions of electroweak theory, flavor physics, and QCD, and exploring new physics BSM. After an upgrade and increase of beam energy, CEPC will be capable of top-quark pair production and could also be converted into a proton-proton machine in the future. CEPC is currently at the stage of the technical design of the accelerator being accomplished and the baseline detector configuration being close to completion. It is expected that the CEPC project will be submitted to the Chinese government for approval in the fall of 2025, and a decision will be made in early 2026.

The JINR group has a strong interest in participating in experiments at CEPC and a wealth of experience in this field, gained in the ATLAS and CMS experiments at the LHC, as well as at the HERA and LEP accelerators; and in the CDF and BESIII experiments. For several years, the JINR group has been successfully cooperating with the Institute of High Energy Physics of the Chinese Academy of Sciences in the preparation of the program of physics research at CEPC, theoretical support of the forthcoming experiments, and software development. However, the possibility of starting the realization of the CEPC project from 2026 and the related preparation for the establishment of international collaborations of experiments at CEPC require the increase of JINR participation in the project.

This project is a continuation and development of the project No. 02-2-1151-1-2025/2025 “Development of a particle registration technique in future experiments with the participation of JINR” within the framework of the JINR Topical Plan for 2025 with specific goals and objectives, including the development of a physics program for performing the tasks of the CEPC experiments.

*The aim of this project is to make proposals for the physics research program, to participate in software and computing development, and to carry out a series of detector R&D aimed at further use in CEPC. Thus, during the next two years, laying a keystone for future full-fledged participation of JINR in experiments at CEPC, provided the construction of this accelerator is approved by the Chinese government.*

## 2.2. Scientific justification (purpose, relevance and scientific novelty, methods and approaches, methodologies, expected results, risks)

### Purpose

The SM of particle physics is a theory that describes with high precision an enormous amount of independent physical observables. At the same time, SM is believed to be an effective low-energy approximation of a more fundamental theory. Besides the fact that there should be new physical phenomena at higher energy scales, there remain many questions about the SM itself, first of all on the origin of the Higgs mechanism. The discovery of the spin-zero Higgs boson in 2012 marked the beginning of a new era in particle physics and at the same time exacerbated new questions. Obviously, resolving these issues will require further experimental and theoretical studies at the electroweak energy scale frontier. Precise measurement of the properties of the Higgs boson, of the top quark, and of all other parameters of the SM will be the major goal in high-energy physics in the coming decades. Direct discovery of BSM physics would be a great success, but also its indirect exploration via observation of deviations from SM expectations is of ultimate importance.

### Relevance and scientific novelty

The HL-LHC will measure the Higgs boson production cross sections with an accuracy of about 5%. Probing new physics well beyond the LHC's reach will require measurements of the Higgs boson's properties to sub-percentage-level precision. To achieve such precision, we will need new instruments such as the proposed electron-positron colliders, the Circular Electron-Positron Collider (CEPC) in China and the Future Electron-Positron Collider (FCC-ee) at CERN, which are Higgs boson factories. The CEPC will operate at center-of-mass energies of  $\sqrt{s}=240$  GeV, around 91.2 GeV, around 160 GeV and, after upgrade, at  $\sim 360$  GeV, acting as a Higgs factory, Z factory, WW threshold scan, and a top quark factory, respectively.

Scientific programs for future colliders, including CEPC, are well developed. The main goals are study of Higgs boson physics, high-precision measurements at the Z pole energy, study of top quark physics, and searches for new physics phenomena [1–4].

The Higgs boson provides a unique, sensitive probe of physics BSM, which may manifest itself as observable deviations in the Higgs boson couplings relative to the SM expectations. At the CEPC, most Higgs boson couplings can be measured with precision at a sub-percent level. The CEPC will be able to measure many of the key Higgs boson properties, such as the total width and decay branching ratios, in a model-independent way, greatly enhancing the coverage of new physics searches. The clean event environment of the CEPC will allow the detailed study of known decay modes and the identification of potential unknown decay modes that are impractical to test at the LHC. A comparison with the HL-LHC is only possible with model-dependent assumptions (see Figure 1). Even with this set of restrictive assumptions, the advantage of the CEPC is still significant. The measurement of  $\kappa_Z$  is more than a factor of 10 better. The CEPC can also significantly improve the precision on a set of  $\kappa$  parameters that are affected by large backgrounds at the LHC, such as  $\kappa_b$ ,  $\kappa_c$ , and  $\kappa_g$ . The direct search for the Higgs boson decay to invisible particles from BSM physics is well motivated and closely connected to the dark sectors.

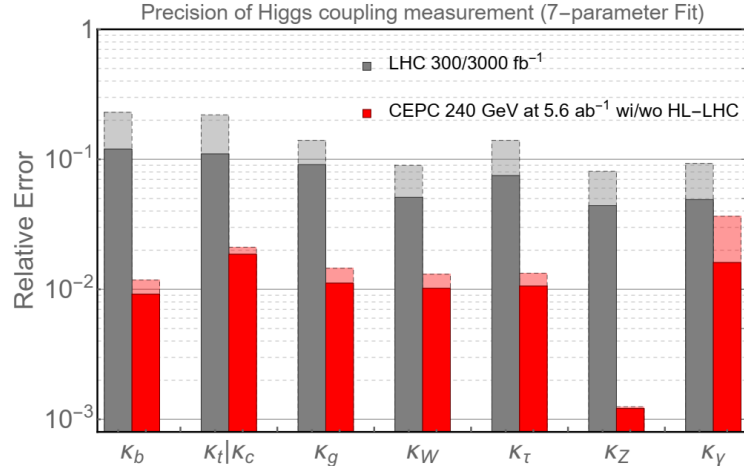


Figure 1. The coupling measurement precision for the CEPC and the HL-LHC [5]. The projections for the CEPC at 240 GeV with an integrated luminosity of  $5.6 \text{ ab}^{-1}$  are shown. The CEPC results without combination with the HL-LHC input are shown as light red bars. The LHC projections for an integrated luminosity of  $300 \text{ fb}^{-1}$  are shown in light gray bars.

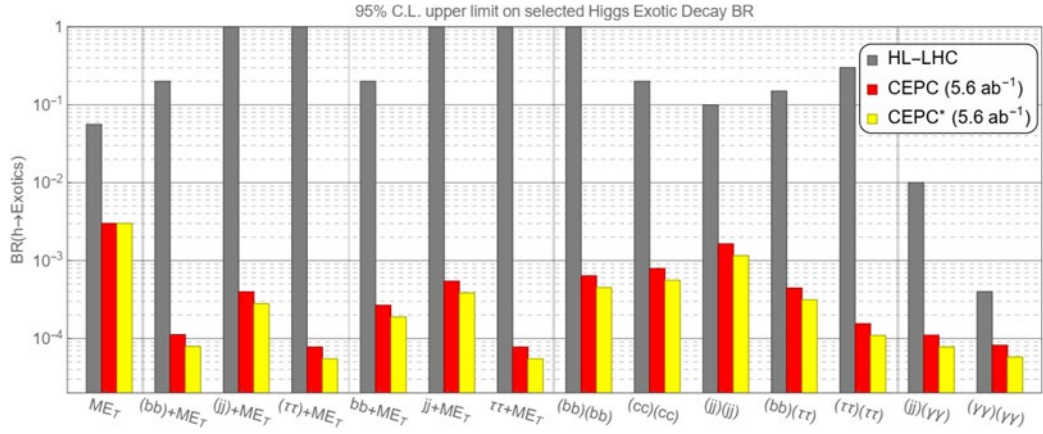


Figure 2. The 95% C.L. upper limits on selected Higgs boson exotic decay branching ratios at the HL-LHC and the CEPC [10]. The red bars correspond to the results using a leptonically decaying spectator Z-boson alone. The yellow bars further include extrapolation with the inclusion of the hadronically decaying Z-bosons.

The Higgs boson can be an important portal to new BSM physics. Such new physics could manifest itself through the exotic decays of the Higgs boson if some of the degrees of freedom are light. The Higgs boson BSM decays have a rich variety of possibilities. Two-particle decays of the Higgs boson into BSM particles,  $H \rightarrow X_1 X_2$ , are considered, where the BSM particles  $X_i$  can subsequently decay. These processes are well-motivated by BSM models such as singlet extensions of the SM, two-Higgs-doublet models, SUSY models, Higgs portals, gauge extensions of the SM, and so on [6–8]. For the Higgs boson decaying into long-lived particles, novel search strategies have to be developed in the future, using also the latest advances in detector development [9]. Selected results for channels, which are hard to constrain at the LHC presented in Figure 2. In comparison with the HL-LHC, the improvement on the Higgs boson exotic decay branching ratios is significant, varying from one to four orders of magnitude for the channels considered. For

the Higgs boson exotic decays into hadronic final states plus missing energy,  $bb+ME_T$ ,  $jj+ME_T$  and  $\tau^+\tau^-+ME_T$ , the CEPC improves the HL-LHC sensitivity by three to four orders of magnitude.

## Methods and approaches

### CEPC Accelerator

The accelerator is a 100-km double-ring collider with two beam interaction points and a synchrotron radiation power of 30 MW as a baseline, with the possibility of upgrading to 50 MW and operating at higher center-of-mass energies up to 360 GeV to produce top-quark pairs [11]. The cross section of the tunnel is 6 meters wide and 5 meters high, allowing the booster, CEPC, and future SppC to be housed in the same tunnel. The collider is designed to operate at center-of-mass energies of 240 GeV (Higgs boson factory), about 91.2 GeV (Z factory), about 160 GeV (WW threshold scan), and a possible upgrade to 360 GeV (top-quark pair). The facility is expected to produce large samples of Higgs bosons ( $\sim 4M$ ), WW ( $\sim 20M$ ), and Z ( $\sim 4T$ ), allowing their properties to be measured with unprecedented precision and to explore physics beyond the SM up to 10 TeV.

### CEPC Detectors

At present, the designs of the two detectors to be installed at the CEPC collider interaction points have not been finalized yet. Instead, a few possible detector configurations are being considered, the choice between which will be made later, at the stage of establishing the experiment's collaboration and technical design of the detector setups, according to available technologies and results of R&D studies.

The CEPC detector concept is based on the high-performance requirements necessary to implement the precision physics program associated with SM tests and the search for new physics phenomena over a wide range of center-of-mass energy and at high beam luminosity. These requirements include large and well-defined solid angle acceptance, excellent particle identification, accurate particle energy and momentum measurements, precise vertex reconstruction, excellent jet reconstruction, and flavor tagging. The physics program requires that all possible final states from decays of intermediate vector bosons, W and Z, and Higgs bosons be separately identified and reconstructed at high resolution. In particular, to clearly distinguish between the final states  $H \rightarrow ZZ^* \rightarrow 4j$  and  $H \rightarrow WW \rightarrow 4j$ , the energy resolution of the CEPC calorimetric system for hadronic jets should be better than existing systems. Higgs decays into two photons, and the search for invisible Higgs decays imposes additional requirements on the resolution of energy and missing energy measurements. Measuring the Higgs boson coupling to the charmed quark requires CEPC detectors to distinguish b-jets, c-jets, and light jets from each other, with high efficiency. The sensitivity to Higgs decays to muon pairs requires high momentum resolution. The latter two demands define the requirements for the vertex detector and tracking system.

The CEPC conceptual design [1] contains three possible detector configurations. The basic CEPC detector concept was developed based on the ILD detector concept of the ILC project, optimized for CEPC conditions. It uses an ultra-high granular calorimetry system to efficiently separate the final state particle showers, a low material tracking system to minimize final state particle interactions, and a 3 Tesla solenoid that surrounds the entire calorimetric system. Two variants of the track system are considered. The default option is a combination of a silicon tracker and a time projection chamber (TPC). The other option is an all-silicon tracker. An alternative detector concept, IDEA, uses a dual-readout calorimeter to achieve excellent energy resolution for both electromagnetic and hadronic showers. Compared to the baseline detector, IDEA has a lower

solenoidal field of 2 Tesla, but is compensated by the large volume of the track system. IDEA has also been proposed as a reference detector for FCC-ee studies [12].

In addition, a new PFA calorimeter-based detector design has recently been developed to further improve the boson mass resolution from 4% to 3% [13]. The basic idea is to use long crystals for ECAL to obtain a much better electromagnetic resolution ( $\sim 3\%/\sqrt{E}$ ), and to use a high-density scintillating glass as the active material of HCAL to achieve a better sampling factor and hence better hadronic energy resolution ( $\sim 40\%/\sqrt{E}$ ). The main goal of the PFA calorimeter system is to achieve a jet energy resolution of about  $30\text{-}40\%/\sqrt{E}$  to meet the requirements of the physics program. Combining a silicon tracker with a TPC or a drift chamber allows improving the charged track momentum resolution and achieving better particle identification ( $\sim 3$  sigma  $\pi/K$  separation for momentum up to 20 GeV/c).

## Methodologies

Work on project 1151 began in 2025 and the main directions will be continued in the coming years. The methods used and the results obtained are presented below.

The possibilities of improving the basic characteristics of electromagnetic calorimeters of the shashlik type under conditions of limited efficiency of wavelength-shifting (WLS) fibers were investigated. For this purpose, a systematic Monte Carlo study was carried out within the framework of the developed model of the basic characteristics of the electromagnetic calorimeter of the “shashlik” type, which, in particular, can be used in the SPD experiment at the NICA collider. The Pb-scintillator calorimeter model uses fibers with a short attenuation length. This leads to deterioration in the linearity of the response and energy resolution of the electromagnetic calorimeter. To improve the performance of such electromagnetic calorimeters, an innovative method has been proposed that uses an ordered arrangement of scintillation plates in order of decreasing light collection efficiency. Using the Monte Carlo model, it is shown that this method can significantly improve the linearity of the response (Figure 3) and the energy resolution of the electromagnetic calorimeter for electron beams and gamma quanta with energies from 0.05 to 8 GeV. Figure 1 shows a comparison of ideal fiber (no attenuation), Kuraray Y11 and OLS-8. The proposed method allows, in conditions of a limited instrumental base, to reduce financial costs for the production of an electromagnetic calorimeter while improving its basic characteristics.

Based on the results of this study, an article was prepared for submission to a journal, the results were reported at the IX SPD collaboration meeting 12-16 May 2025, in Yerevan, Armenia.

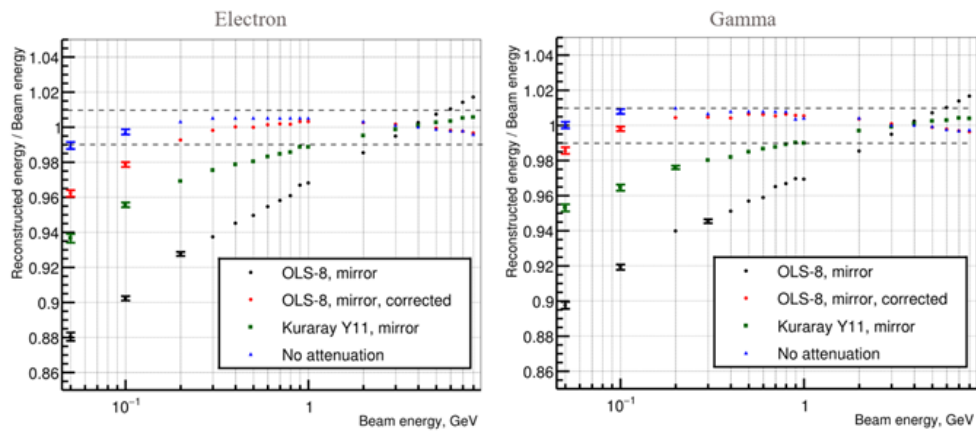


Figure 3. Linearity of the electromagnetic calorimeter module response with and without the correction model for electron (left) and gamma-ray (right) irradiation cases as a function of beam energy.

As part of the study of radiation hardness of inorganic scintillators, the effect of gamma irradiation on BaF<sub>2</sub> is being studied. The studied samples are crystals of pure and yttrium-doped barium fluoride in the form of a cube with dimensions of 10x10x10 mm<sup>3</sup>. All faces of the samples are optically polished. For the experiment, 24 samples were selected and divided into 6 groups, each of which consisted of a pure sample and doped samples with an yttrium content of 1, 3 and 5 mole percent. The characteristics of the samples were measured before and after irradiation at the gamma-irradiation complex at the Institute of Radiation Problems (Baku) with a radioactive source of <sup>60</sup>Co with a total activity at the time of irradiation of 3586.5 Ci. The samples were measured for the total light output within 3 μs after the start of the scintillation flash, the light output of the fast component of the flash in the first 20 ns, and the energy resolution when registering gamma quanta with an energy of 51 keV from a <sup>22</sup>Na source. The light transmittance of the samples was also measured in the wavelength range of 200-600 nm.

Each group of samples was irradiated to the corresponding absorbed dose: 29 rad, 290 rad, 2.9 krad, 29 krad, 2.9 Mrad in alanine equivalent. To calculate the true values of the absorbed doses by the crystals, computer simulation was carried out using the real geometry of the gamma-irradiation complex. The simulation results showed that the dose rate conversion factor for barium fluoride relative to alanine is 1.25 and the actual absorbed dose values for each group of samples were 36 rad, 360 rad, 3.6 krad, 36 krad, 360 krad, 3.6 Mrad, respectively.

The results of the study show that after irradiation the light outputs of all samples decrease. The behavior of the fast component of the luminescence is of greatest interest. The ratio of the fast component of the emission to the total signal after irradiation decreases for all samples, but the greatest decrease is demonstrated by samples with 3% yttrium doping. These same samples have the greatest drop in the light yield of the fast component, which can be seen in Fig. 4. This result coincides with the loss of light yields of similar samples that we observed earlier after irradiation with the neutron beam of the IBR-2M reactor.

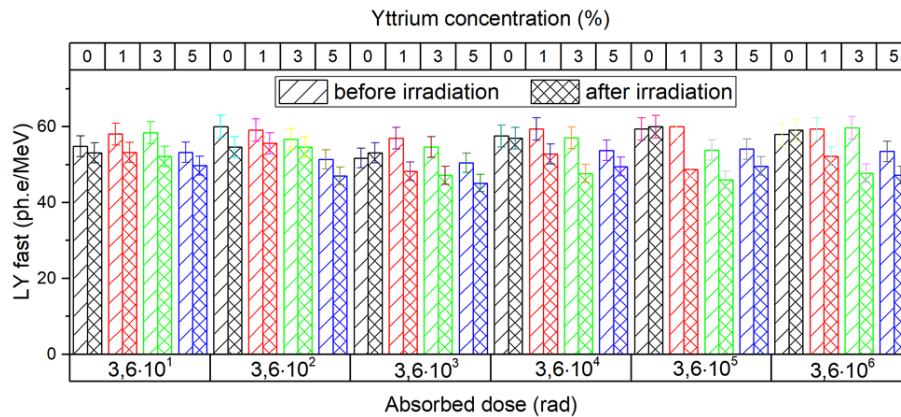


Fig. 4. Light yields of the fast emission component of all samples before and after irradiation, in photoelectrons/MeV.

Preliminary results of these studies were presented at the session-conference of the Nuclear Physics Section of the Physical Sciences Department of the Russian Academy of Sciences in February 2025 (Moscow). We are currently preparing an article for submission to a journal

A study was conducted on the influence of gamma radiation on the properties of GaN transistors and amplifiers for SiPM based on them. Power GaN transistors IGLR60R260D1 manufactured by Infineon (Germany) were used as the studied samples. The samples were irradiated with a gamma source <sup>60</sup>Co with doses up to 3 Mrad.

Fig. 5 shows a comparative analysis of the characteristics of transistors before and after irradiation, as well as a comparison of these characteristics with the circuit model.

From non-irradiated and irradiated transistors, amplifiers developed for EQR20 11-6060D-S SiPM were manufactured, for which measurements and comparison of the frequency response,

frequency band and noise spectra were carried out (Fig. 6). The study showed sufficient radiation hardness of the selected GaN transistors at an absorbed dose of up to  $\sim 3$  Mrad. This allows us to propose using GaN as a promising radiation-resistant material for developing amplifiers for modern high-load detectors.

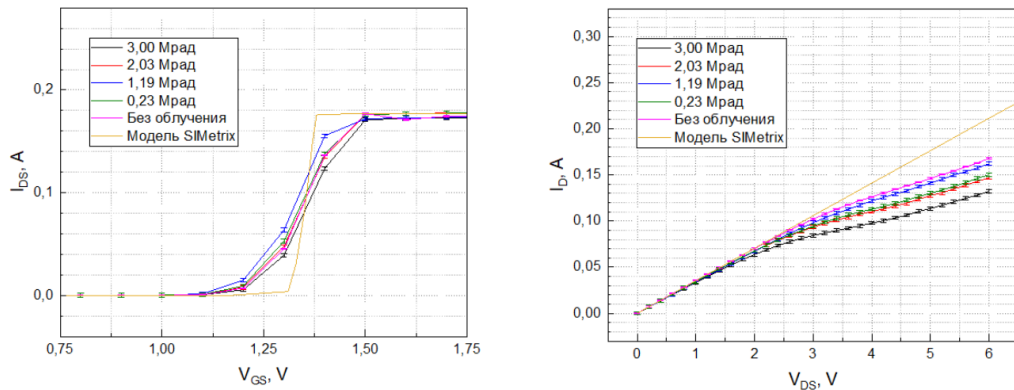


Fig. 5. Transfer and output characteristics of the transistor. For the transfer characteristic  $V_{DS}=5$  V, for the output characteristic  $V_{GS}=1.3$  V.

Preliminary results of this study were presented at the Session-Conference of the Nuclear Physics Section of the Physical Sciences Department of the Russian Academy of Sciences. A publication on the topic of the study is currently being prepared.

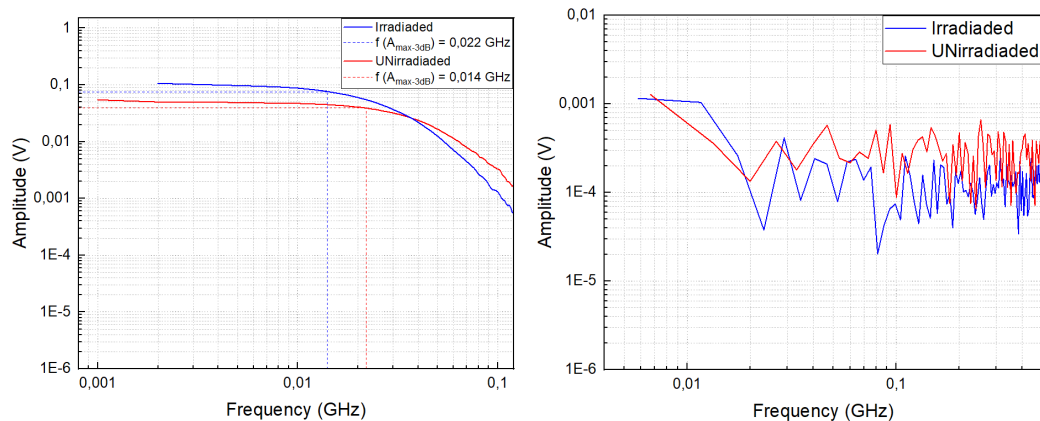


Fig. 6. Comparison of the frequency response and noise spectrum of amplifiers made of irradiated and non-irradiated transistors.

As part of the work with microstructured gas detectors, test boards with a resistive coating of diamond-like carbon (DLC) were developed and manufactured for the production of Micromegas detectors. Based on these boards, prototypes of Micromegas detectors were produced to conduct an experiment on the accumulation of multiple breakdown events (about 100 million per  $\text{cm}^2$ ) and study their influence on the characteristics of a detector with a resistive anode made of DLC coating.

At the experimental stand of the DLNP of JINR, tests of such prototypes for the accumulation of multiple breakdowns from highly ionizing particles were carried out. The robustness of the microstructure detector with a resistive anode made of DLC coating to multiple breakdown events and the possibility of its application under conditions of high rate of highly ionizing particles (for example, the conditions expected in the internal tracker of the SPD experiment) are demonstrated. A publication is being prepared based on the obtained results.

Flexible polyimide boards with a thickness of  $50 \mu\text{m}$  with reading electrodes were developed and manufactured for the production of a prototype of a microstructure gas-discharge detector using Bulk MicroMegas technology with a small amount of substance. The detector

design has been developed, a prototype detector model has been manufactured, and the production and testing of a detector prototype using Bulk MicroMegas technology with a small amount of substance is being prepared. A method for creating a microstructural dielectric pattern for insulating an anode high-voltage mesh electrode using a photolithography method for manufacturing a well-type electron multiplier with a resistive anode (RWELL) has been developed. A prototype of such a detector with an insulating microstructure for a mesh high-voltage electrode has been manufactured. The prototype is being tested.

In muon systems of modern facilities, long scintillation strips with signal readout using wavelength-shifting fibers are often used. Strips can have different cross-section geometries and fiber placement methods. An important task is to reliably register signals from long counters and to ensure high efficiency when a muon passes through any point of the strip cross-section. These studies are being conducted this year and will be continued in the following years.

We have made a cross-sectional scan of a strip of triangular cross-section on cosmic muons. The strip cross-section has the shape of a right triangle with a base of 33 mm and a height of 17 mm, the fiber is inserted into a longitudinal hole in the center of the strip. The common trigger from cosmic muons was switched on by the coincidence of two scintillation counters measuring  $80 \times 80 \times 10 \text{ mm}^3$ . The 10 mm thickness of the trigger counters determined the size of the region along the strip where passing muons were recorded. The muons were recorded by a track detector consisting of two 32-channel hodoscopes with Kuraray SCSF-81J scintillation fibers with a cross-section of  $2 \times 2 \text{ mm}^2$  (left part of Figure 7). The light is collected using a matrix of 16 SiPM SensL MicroFJ-SMA-30020 with a working surface of  $3 \times 3 \text{ mm}^2$ .

A long-term data acquisition was performed, with approximately 36,000 events collected. During the data analysis, vertically passing muons were selected from the total number by selecting signal matches from the corresponding fibers from the upper and lower hodoscopes. This approach allowed us to select cosmic muons with a divergence of  $\pm 0.04$  radians (2.3 degrees) across the strip and  $\pm 0.11$  radians (6.5 degrees) along the strip. On average, about 120 events were selected per position, or approximately 3.5 thousand events out of 36 thousand collected.

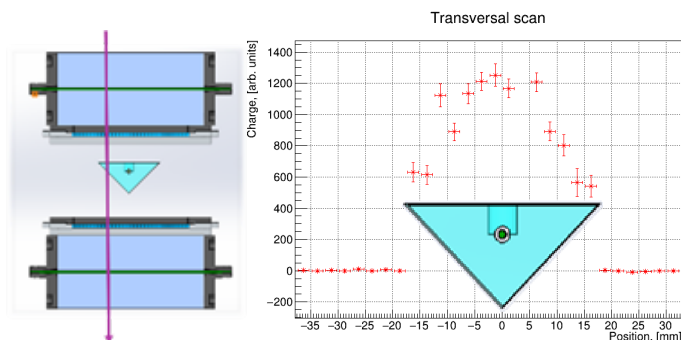


Fig. 7. View of the assembly during data acquisition on cosmic muons (left) and preliminary result of the cross-section scan of the triangular cross-section strip (right)

Based on the obtained results for light collection from the passage of muons, the dependence of light collection on the position across the strip was obtained (right part of Fig. 7). Further plans for strip research include studying the light collection and attenuation length of rectangular strips with different fiber locations and diameters.

The project involved modeling thick heterogeneous neutron detectors. A composite was considered that included grains of the lithium-containing glass scintillator NE 912 in a supporting optical binder. The aim of the study was to determine the maximum neutron conversion efficiency and the minimum  $\gamma$ -sensitivity of the detector with variations in the composite structure parameters – grain size, glass concentration and total thickness. A Monte Carlo simulation computer program was developed to calculate the energy transferred to the scintillator during exposure to thermal neutrons and  $\gamma$ -quanta.

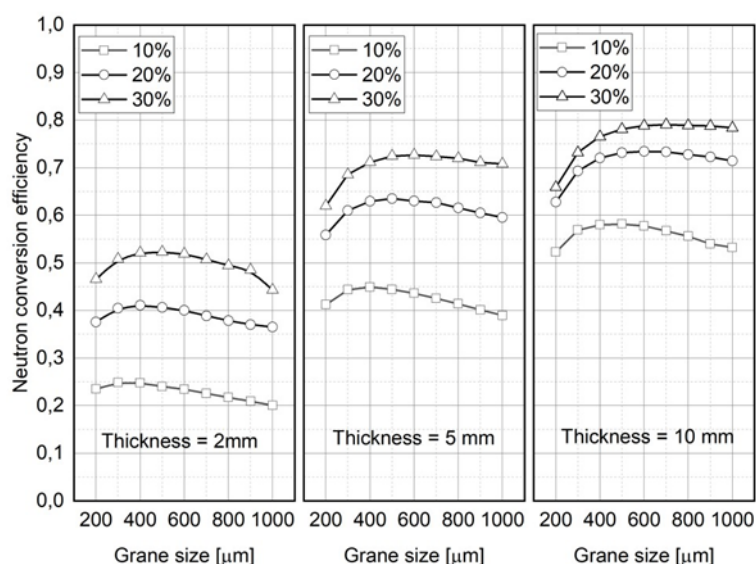


Fig. 8. Dependence of neutron conversion efficiency on grain size for scintillator thicknesses of 2, 5 and 10 mm. Glass scintillator grain concentrations: 10, 20 and 30%.

Simulation showed that the neutron conversion efficiency has a maximum in the grain size range from 400 to 500  $\mu\text{m}$  for thin composites and low concentrations of NE 912 (Fig. 8). With a compromise value of neutron conversion efficiency equal to 0.7 for a composite with a thickness of 15 mm, it is possible to obtain  $\gamma$ -sensitivity at the level of  $S=7 \times 10^{-8}$ , an order of magnitude lower than that of NE 912 with a thickness of 1 mm.

Within the framework of the project, samples of neutron scintillators were developed and created based on zinc sulfide, lithium fluoride and boron oxide crystals produced in Russia (Luminofor, Stavropol). At present, the transparency measurements of the produced samples have been carried out. Further studies will be carried out on the thermal neutron beam of the IBR-2M reactor.

Preliminary results of simulation were presented at the session-conference of the Nuclear Physics Section of the Physical Sciences Department of the Russian Academy of Sciences. The work is currently prepared for publication. The studies of heterogeneous neutron detectors will be completed in 2025.

Straw tubes are single-coordinate wire detectors. The coordinate of the particle passage is determined by the electron drift time, and orthogonally located tubes are usually used to determine the second coordinate along the wire. We conduct research on straw tubes, obtaining information about the coordinate along the wire using induced signals on the segmented cathode surfaces of straw detectors. A previously manufactured and tested prototype of a straw detector with stripes on the outer surface of the cathode (Fig. 9, left) demonstrated the possibility of obtaining information about the coordinate along the detector using the center of gravity of the charge with a high accuracy of up to 100  $\mu\text{m}$ . In this case, the inner surface of the cathode must have finite conductivity to be able to register the induced charge on the outer strips. The disadvantage of this method and design is the large amount of electronics and the difficulty of connecting contacts to the segments of the thin-walled cathode tube. To reduce the number of channels, we proposed a two-stage method for determining coordinates along the straw detector using the "double wedge" method. The inner part of the cathode has a weakly conductive coating based on graphite with a resistance of 3 kOhm/square and is divided along the length into two wedges. The outer surface of the cathode has a gold coating, divided into two parts with a repeating "double wedge" structure with a pitch of 27 mm (Fig. 9, right). The charge ratio on the internal wedges determines the coordinate of the particle's passage with low resolution, and data from the external cathode wedges will allow an accuracy of better than 0.5 mm to be obtained.

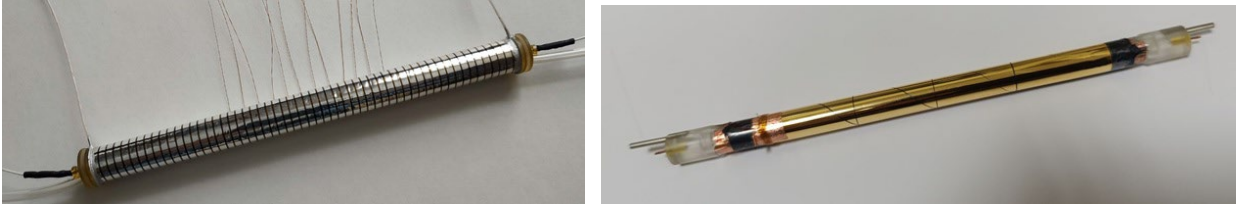


Fig. 9. Two-coordinate straw detectors with a segmented strip cathode (left) and with a “double wedge” cathode (right).

The first tests of the manufactured prototype have begun. The results showed a strong influence of the internal and external cathode electrodes on each other. Apparently, the capacitive coupling of the electrodes distorts the signals. Despite this, the method looks very promising and we plan to continue this work.

*Work on developing methods for calibrating electromagnetic and hadron calorimeters, studying the radiation hardness of inorganic scintillators and electronic elements, creating prototypes of calorimeters and studying their parameters, optimizing muon system detectors, and developing microstructural gas detectors will be continued within the framework of the project.*

*Below are the work plans for the project.*

### 1. Development of the experimental program

A physics performance study of several physics topics will be performed for CEPC using Monte Carlo simulation, and the relevant analysis procedures will be elaborated.

The Higgs boson physics is the main task of the experiments at CEPC for all 10 years of data collection. The processes occurring with the formation of the Higgs boson at the CEPC at the energy  $\sqrt{s} \sim 240\text{--}250$  GeV are  $e^+e^- \rightarrow ZH$ ,  $e^+e^- \rightarrow \nu\bar{\nu}H$ , and  $e^+e^- \rightarrow e^+e^-H$ . Higgs boson candidates can be identified using a mass recoil method, without labeling their decays. The branching ratios of the Higgs boson decay can be determined by studying its individual decay modes. Higgs boson decays, which can be identified by their unique signatures, will be studied in the following modes:  $H \rightarrow b\bar{b}/c\bar{c}/gg$ ,  $H \rightarrow WW^*$ ,  $H \rightarrow WZ^*$ ,  $H \rightarrow W\gamma$ ,  $H \rightarrow \tau^+\tau^-$ ,  $H \rightarrow \mu^+\mu^-$ ,  $H \rightarrow inv$ . A systematic study of the  $e^+e^- \rightarrow ZX$  processes will be carried out with the aim of determining the properties of the Higgs bosons with the best possible accuracy and new physics BSM searches using Monte Carlo generations for full detector simulations of signal and background events. As a result, algorithms will be developed for the best signal-to-background ratio in the selected events. Based on this analysis, values of the Higgs boson characteristics are expected to be obtained with accuracy an order of magnitude better than in the experiments at the HL-LHC, and new physics phenomena BSM will be discovered.

A large sample of  $B_s^0$  and  $B_c^+$  mesons allows us to measure CP-violating phase  $\phi_s$  in decay  $B_s^0 \rightarrow J/\psi \phi(1020)$  with unprecedented accuracy. The excellent particle identification, accurate track and vertex reconstruction, and extensive geometric acceptance of the planned detectors at the CEPC will make it possible to measure the phase  $\phi_s$  in another  $B_s^0$  decay channel  $B_s^0 \rightarrow J/\psi \pi^+ \pi^-$ .

Besides this, there is considerable interest in the processes occurring with the formation of heavy ( $c$ ,  $b$ ) flavors and their bound states in  $e^+e^-$  annihilation in general. Such processes, in particular, are background for many processes of new physics BSM, which will be studied at the CEPC. Their cross sections are huge; for example, near the  $Z$ -boson mass, they are two orders of magnitude larger than the cross section of the process  $e^+e^- \rightarrow e^+e^-Z$ . It is important that direct information on the fragmentation functions of heavy quarks into mesons can be obtained as a result of precision measurements of the total and differential cross sections for the production of  $D$  and  $B$  mesons in  $e^+e^-$  annihilation, which will allow us to qualitatively improve the accuracy of measuring the fragmentation functions. Experimental studies of reactions in collisions of virtual

photons produced in  $e^+e^-$  interactions, along with the study of the processes of formation of bound states of heavy quarks (quarkonia), will allow us to obtain information on the dynamics of the quark-gluon interaction in a new kinematic region. It is by studying these reactions that we can extract new information on the behavior of electromagnetic form factors in the time-like region of transferred momenta,  $Q^2 > 0$ .

Finally, two photon collisions offer a variety of physics phenomena that can be studied at future electron-positron colliders [14]. Using the planned CEPC parameters as a benchmark, we will consider several topics within two-photon collisions. With the fully integrated luminosity, Higgs boson photoproduction can be reliably observed, and large statistics on various quarkonium states can be collected. The LEP results for the photon structure function and tau lepton anomalous magnetic moment can be improved by 1-2 orders of magnitude.

## 2. High-precision theory calculations, theory support of experiments

The theoretical support of the collider experiments focuses on precision modeling of processes in electron-positron accelerators, achieving accuracy up to the two-loop level. The JINR group already has a significant experience in theoretical support for experiments in high-energy physics: ZFITTER (LEP1, LEP2) and HECTOR (HERA). The integrator MCSANC and generator ReneSANCe are used in the analysis of Drell-Yan data in the ATLAS experiment.

The SANC (Support for Analytic and Numeric Computations) system, developed by the JINR group, is already widely used for calculations in the scope of CEPC physics studies [15-19]. However, further enhancements are necessary, implementing new processes within the computational framework, evaluating corrections beyond the leading order, and incorporating polarization effects into the modeling process. In the scope of this project, the development will be focused on the following studies:

- Theoretical support for luminosity estimation. Precision measurement of the Higgs boson mass.
- Measurement of the top quark polarization and determination of the anomalous top quark form-factors.
- The development of the Monte Carlo generator ReneSANCe, taking into account initial and final polarization states for the processes  $e^+e^- \rightarrow e^+e^- (\mu\mu, \tau\tau, t\bar{t}, HZ, H\gamma, ZZ, Z\gamma, H\mu\mu, Hv\nu, f\bar{f}\gamma, \gamma\gamma), \gamma\gamma \rightarrow \gamma\gamma(Z\gamma, ZZ)$ .
- Development of additional building blocks of the higher-order radiative corrections.

## 3. Software and computing

The significant amount of data to be produced at CEPC requires a large distributed computing infrastructure for data storage and data processing. Moreover, this infrastructure will be needed long before the data taking starts due to the large-scale simulation needed for the development of the experimental program and performance studies. Based on the experience gained in the ATLAS experiment and in the design of the computing system for NICA/SPD, the JINR group is going to participate in the design, development, and commissioning of the CEPC computing system. Options for JINR joining the CEPC computing, possibly integrating with the NICA data processing system, will be worked out. Participation in the simulation of physics processes, modeling detectors, and developing algorithms and offline software for the experiments at CEPC is planned as well.

#### 4. Detector R&D

A calorimetry system is employed in the CEPC detectors to provide hermetic coverage for high-resolution energy measurements of electrons, photons, taus, and hadronic jets. Two different approaches are used for the CEPC calorimetry system. The first one is aimed at measuring individual particles in a jet using a calorimetry system with a very high granularity based on the particle flow algorithm (PFA), and the second one is aimed at a homogeneous and integrated solution based on the dual-readout concept.

To distinguish the hadronic decays of W and Z bosons, a 3–4% invariant mass resolution for two-jet systems is required. Such a performance needs a jet energy resolution of  $\sim 30\%/\sqrt{E}$ , at energies below 100 GeV.

A PFA-based high-granularity HCAL with scintillation glass/absorber steel is proposed as a baseline detector for the CEPC. Scintillation glass has a density of about  $6.0 \text{ g/cm}^3$ , a light yield of more than 1000 photons/MeV, and a decay time of more than 100 ns. There are no technologies yet for producing large-size samples (more than  $10 \times 10 \text{ cm}^2$ ). The HCAL has 48 layers of steel absorbers/scintillation glass tiles with a total depth of  $6\lambda_I$ , as shown in Fig. 10. The scintillation layer consists of glass tiles measuring  $4 \times 4 \times 1 \text{ cm}^3$ .

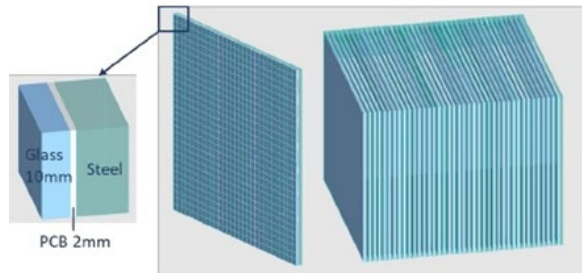


Figure 10. The HCAL module has 48 layers of steel absorbers/scintillation glass tiles; the total depth is  $6\lambda_I$ .

A calorimeter based on the beryllium germanium oxide (BGO) crystals is considered as the baseline ECAL design (BSO crystals are considered as an alternative option). The length of the ECAL barrel is 580 cm, and the inner and outer diameters are 366 cm and 426 cm. The barrel is composed of individual modules of trapezoid shapes. The endcap modules are made from  $1 \times 1 \times 40 \text{ cm}^3$  BGO crystal bars arranged orthogonally in every two layers, providing fine segmentation. The modules have a thickness of 24 radiation lengths. The ECAL endcap module schematic is presented in Figure 11.

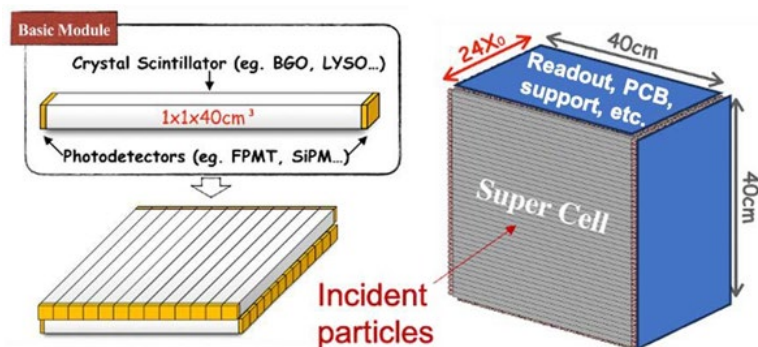


Figure 11. ECAL endcap module schematic.

10x10x400 mm<sup>3</sup> BGO crystal bars provide 10x10 mm<sup>2</sup> transverse granularity. An alternative option of using crystals measuring 15x15x400 mm<sup>3</sup> is currently being considered. This option significantly reduces the total readout channels, saves costs on electronics and SiPM, and greatly decreases power dissipation. However, this leads to some degradation of the ECAL parameters. The Higgs decay into two photons,  $H \rightarrow \gamma\gamma$ , is a physical criterion that is crucial for ECAL. 15 mm granularity shows slightly degraded performance in gamma separation efficiency.  $\pi^0$  performance is degraded in high energy with a 15x15 mm<sup>2</sup> crystal cross-section but can be improved by the  $\gamma/\pi^0$  discrimination technique. Further simulation of the ECAL calorimeter and prototype testing are required to optimize performance. In addition, it is necessary to conduct studies on the radiation hardness of the BGO crystals.

The project participants have extensive experience in the simulation, creation, characterization, and maintenance of electromagnetic and hadron calorimeters [20], in the development of various methods for calibrating of calorimeters [21, 22], in the characterization of crystals and crystal calorimeters [23], and in the study of their radiation resistance [24]. All these stages will be completed during the project, including development of calorimeter calibration methods, full simulation of the calorimeter system, production of prototypes, and their testing on benches and in accelerator beams.

Outside the solenoid is an iron yoke serving as the magnetic flux return. The yoke will be instrumented with a muon detector designed for muon identification. However, it could also be used to detect the leakage of HCAL and can be used for trigger and other tasks. The muon detector should provide solid angle coverage of  $0.98 \times 4\pi$ , detection efficiency  $>95\%$ , position resolution  $\sim 1$  cm, and time resolution  $\sim 1$  ns. In the baseline option, the muon detector will use plastic scintillation strips with WLS fibers and SiPM readout. Resistive Plate Chambers (RPC) and microstructural gas  $\mu$ -RWELL detector are also being considered as alternatives.

Extruded plastic scintillator technology will be used to produce scintillator strips. Various strip designs are being considered: rectangular, square, or triangular cross-sections with fibers glued into grooves or placed into holes inside the scintillation strips (Figure 12). The scintillation strips are assembled into superlayers in orthogonal directions (X, Y), and two superlayers (each approximately half the length of the yoke) are inserted into each gap between the iron layers.

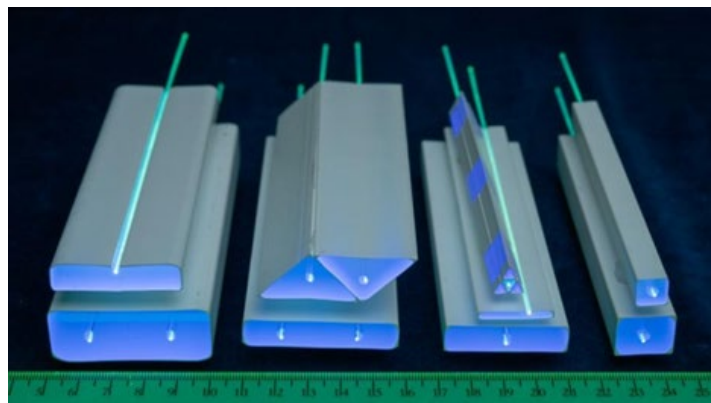


Figure 12. Scintillation strips with WLS fibers as candidates for use in the muon system.

To improve the characteristics of the muon detector and select the optimal detector parameters, additional simulation and testing of prototypes is required. Currently, a strip with a cross-section of 10x40 mm<sup>2</sup> with a fiber glued in a groove is the basic option. To increase light

collection from strips, options for using larger-diameter WLS fibers are being considered. Various prototypes with these options will be simulated, created, and tested. The project participants have extensive experience in the development and characterization of muon systems based on the long scintillation strips with WLS fiber readout [25, 26].

The CEPC Tracking Detector System uses silicon vertex detectors in combination with a gas detector to track and identify particles (PID). The Time Projection Chamber (TPC) is the default outer tracker option of the CEPC baseline detector concept.

The TPC has a cylindrical drift volume with an inner radius of 0.63 m, an outer radius of 1.8 m, and a full length of 4.7 m. The central cathode plane is held at a potential of 50 kV, and the two anodes at the two end plates are at ground potential, with a highly homogeneous electrical field of 300 V/cm between the electrodes. The drift volume is filled with Ar/CF<sub>4</sub>/i-C<sub>4</sub>H<sub>10</sub> in the ratio of 95%/3%/2%. The CEPC TPC will operate at atmospheric pressure, providing a material budget of less than 1% $X_0$  in the central region.

Signal acquisition from TPC using pixelated Micromegas detector is the basic in CEPC. It can provide <3%  $dN/dx$  resolution by cluster counting and 5.4%  $dE/dx$  resolution by charge measurement. Preliminary simulation results show that  $3\sigma$   $\pi/K$  separation at 20 GeV with a 50 cm drift distance can be achieved. However, some key issues should be modeled and tested on prototypes.

The project participants have extensive experience in the design, creation, and research of Micromegas detectors. We plan to produce prototypes of the Micromegas microstructured gas detector and test them in the CEPC TPC prototype. The JINR group participants have full expertise to fulfill these tasks [27].

## Expected results

The result of the project will be:

- A systematic study of  $e^+e^- \rightarrow ZX$  processes will be carried out with the aim of precisely determining the properties of Higgs bosons and searching for new physical directions for characterizing the SM using Monte Carlo generators.
- Theoretical support for the collider luminosity estimate will be provided.
- The top quark polarization will be simulated and anomalous top quark form factors will be determined. The ReneSANCE Monte Carlo generator will be developed taking into account the initial and final polarization algorithms for the processes  $e^+e^- \rightarrow e^+e^-$  ( $\mu\mu$ ,  $\tau\tau$ ,  $t\bar{t}$ ,  $HZ$ ,  $H\gamma$ ,  $ZZ$ ,  $Z\gamma$ ,  $H\mu\mu$ ,  $H\nu\nu$ ,  $f\bar{f}\gamma$ ,  $\gamma\gamma$ ),  $\gamma\gamma \rightarrow \gamma\gamma$  ( $Z\gamma$ ,  $ZZ$ ).
- The design, development and preparation for commissioning of the CEPC computing system will be carried out, options for connecting JINR to the CEPC computing system with possible integration with the NICA data processing system will be worked out.
- Methods for calibrating electromagnetic and hadronic calorimeters will be developed, modeling of the calorimetric system will be carried out, prototypes will be manufactured and tested on benches and in accelerator beams.
- Various prototypes of the muon detector will be simulated, created and tested, and solutions for creating the detector will be proposed.
- Prototypes of the Micromegas microstructured gas detector will be manufactured and tested in the CEPC TPC prototype.

## Risks

SWOT analysis :

Strengths of the project:

- Extensive experience in simulation methods, development of software and implementation of machine learning in data analysis
- Expertize in developing of various types of innovative detectors and electronics and experience in their use in experiments
- Development of new methods and technologies

Weakness of the project:

- Potential problems with purchasing and obtaining the necessary materials and equipment to complete the project tasks

Opportunities:

- The project provides a prominent role for young scientists and the opportunity to become part of a leading experiment in the coming decades

Threats:

- Major changes in the world situation

## References:

1. CEPC Study Group, CEPC Conceptual Design Report: Volume 2, arXiv: 1811.10545 [hep-ex]
2. F. An, et al., Precision Higgs physics at the CEPC, Chin. Phys. C 43 (2019) 4, 043002
3. X. Ai, et al., Flavor Physics at CEPC: a General Perspective, arXiv:2412.19743 [hep-ex]
4. Y. Zhu, et al., The Higgs $\rightarrow$ bb, cc, gg measurement at CEPC, JHEP 11 (2022) 100
5. ATLAS Collaboration, Projections for measurements of Higgs boson signal strengths and coupling parameters with the ATLAS detector at a HL-LHC, ATL-PHYS-PUB-2014-016 (2014).
6. “Measurement of time-dependent CP violation in  $B_s^0 \rightarrow J/\psi \phi(1020)$  decays with the CMS detector”. In: (2024)
7. Fenfen An, et al., Precision Higgs physics at the CEPC, Chinese Physics C Vol. 43, No. 4 (2019) 043002
8. ATLAS Collaboration, Projections for measurements of Higgs boson signal strengths and coupling parameters with the ATLAS detector at a HL-LHC, ATL-PHYS-PUB-2014-016 (2014)

9. LHC Higgs Cross Section Working Group, Handbook of LHC Higgs Cross Sections: 4. Deciphering the Nature of the Higgs Sector, arXiv:1610.07922 [hep-ph]
10. Z. Liu, L.-T. Wang, and H. Zhang, Exotic decays of the 125 GeV Higgs boson at future  $e^+e^-$  lepton colliders, arXiv:1612.09284 [hep-ph]
11. CEPC Study Group, CEPC Technical Design Report: Accelerator, Radiat. Detect. Technol. Methods 8 (2024) 1, 1-1105, Radiat. Detect. Technol. Methods 9 (2025) 1, 184-192 (erratum)
12. M. Abbrescia, et al., The IDEA detector concept for FCC-ee, arXiv:2502.21223 [physics.ins-det]
13. CEPC Study Group, Status of the CEPC Project, PoS ICHEP2024 (2025) 821
14. I. Boyko, V. Bytev, A. Zhemchugov, Two-photon physics at future electron-positron colliders, Chin. Phys. C 47 (2023) 1, 013001
15. A. Arbuzov, et al., Monte Carlo programs for small-angle Bhabha scattering, Chin. Phys. C 48 (2024) 4, 043002
16. S. Bondarenko, et al., Two-Loop QED/QCD Corrections for the Polarized  $\gamma\gamma\rightarrow\gamma\gamma$  Process in SANCphot, JETP Lett. 120 (2024) 11, 795-799
17. S. Bondarenko, et al., One-loop electroweak radiative corrections to polarized process, Phys. Rev. D 109 (2024) 3, 033012
18. S. Bondarenko, L. Kalinovskaya, A. Saproonov, Monte-Carlo tool SANCphot for polarized  $\gamma\gamma$  collision simulation, Comput. Phys. Commun. 294 (2024) 108929
19. A. Arbuzov, et al., Electroweak Effects in  $e^+e^-\rightarrow ZH$  Process, Symmetry 13 (2021) 7, 1256
20. P. Adragna et al., The ATLAS hadronic tile calorimeter: From construction toward physics; Trans. Nucl. Sci. 53 (2006) 1275-1281
21. Y.A. Kulchitsky, V.B. Vinogradov, Analytical representation of the longitudinal hadronic shower development, NIM A413 (1998) 484-486, hep-ex/9903019
22. ATLAS Collaboration; Results from a new combined test of an electromagnetic liquid argon calorimeter with a hadronic scintillating-tile calorimeter, NIM A 449 (2000) 461-477
23. N. Atanov et al. The Mu2e Crystal Calorimeter: An Overview, Instruments 6 (2022) 4, 60
24. V. Baranov, Yu.I. Davydov, I.I. Vasilyev, Light outputs of yttrium doped BaF<sub>2</sub> crystals irradiated with neutrons, JINST 17 (2022) 01, P01036
25. A. Artikov et al., Photoelectron yields of scintillation counters with embedded wavelength-shifting fibers read out with silicon photomultipliers, NIM A890 (2019), 84-95
26. A. Artikov et al., High efficiency muon registration system based on scintillator strips, NIM A1064 (2024) 169436
27. D. Dedovich et al., Bulk Micromegas fabrication at JINR, JINST 14 (2019) 07, T07004

### 2.3. Estimated completion date

2027

## 2.4. Participating JINR laboratories

DLNP

BLTP

LHEP

MLIT

### 2.4.1. MICC resource requirements

Computing resources	Distribution by year	
	1 <sup>st</sup> year	2 <sup>nd</sup> year
Data storage (TB) - EOS - Tapes	10	20
Tier 1 (CPU core hours)	-	-
Tier 2 (CPU core hours)	20000	20000
SC Govorun (CPU core hours) - CPU - GPU	-	-
Clouds (CPU cores)	-	-

## 2.5. Participating countries, scientific and educational organisations

Organization	Country	City	Participants	Type of agreement
IHEP	China	Beijing	Y.F. Wang M.Q. Ruan W.D. Li X.C. Lou M. Chen	Cooperation Agreement
Shandong University	China	Qingdao	X.T. Huang	Cooperation Agreement
Fudan University	China	Shanghai	X. Wang	Cooperation Agreement
HSE, MIPT	Russia	Moscow	T.A. Aushev P.N. Pakhlov	Cooperation Agreement

PNPI NRC KI	Russia	Gatchina	O.K. Fedin	Cooperation Agreement
BINP RAS	Russia	Novosibirsk	A.Barnyakov	Cooperation Agreement
IP NASB	Belarus	Minsk	Yu.A. Kurochkin	Cooperation Agreement
INP BSU	Belarus	Minsk	O.V. Misevich V.V. Makarenko	Cooperation Agreement
IE NASB	Belarus	Minsk	V.G. Baev	Cooperation Agreement

**2.6. Co-executing organisations** (*those collaborating organisations/partners without whose financial, infrastructural participation the implementation of the research programme is impossible. An example is JINR's participation in the LHC experiments at CERN*).

IHEP CAS

### 3. Staffing

#### 3.1. Staffing needs in the first year of implementation (total number of participants)

No. n/a	Category employee	Core staff Amount of FTE	Associated Personnel Amount of FTE
1.	scientific staff	25.4	0
2.	engineers	1.8	0
3.	professionals	0	0
4.	employees	0	0
5.	workers	0.4	0
<b>Total:</b>		<b>27.6</b>	<b>0</b>

#### 3.2. Human resources available

##### 3.2.1. JINR core staff (total number of participants)

No.	Category of personnel	Full name	Division	Position	Amount of FTE
1.	research scientists	Yuri Davydov	DLNP	Head of department Project leader	0.7
2.		Alexey Zhemchugov	DLNP	Deputy head of department Project leader	0.4
3.		Yuri Kulchitsky	DLNP	Head of sector Deputy project leader	0.7
4		Alexey Guskov	DLNP	Deputy Director	0.1
5		Lidia Kalinovskaya	DLNP	Head of sector	0.8

6		Alexi Gongadze	DLNP	Head of sector	0.4
7		Ivan Eletsikh	DLNP	Head of sector	0.3
8		Gennady Lykasov	DLNP	Chief researcher	0.5
9		Akram Artikov	DLNP	Leading researcher	0.7
10		Igor Boyko	DLNP	Senior researcher	0.7
11		Davit Chokheli	DLNP	Senior researcher	0.6
12		Igor Suslov	DLNP	Senior researcher	0.5
13		Nazim Huseinov	DLNP	Senior researcher	0.5
14		Vladimir Lyubushkin	DLNP	Senior researcher	0.5
15		Aleksandr Simonenko	DLNP	Senior researcher	0.6
16		Leonid Gladilin	DLNP	Senior researcher	0.3
17		Yahor Dydyska	DLNP	Senior researcher	0.8
18		Vitaly Yermolchyk	DLNP	Senior researcher	0.8
19		Andrey Sapronov	DLNP	Senior researcher	0.8
20		Renat Sadykov	DLNP	Senior researcher	0.8
21		Leonid Rumyantsev	DLNP	Senior researcher	0.3
22		Andrey Prokhorov	DLNP	Senior researcher	0.8
23		Roman Lee	DLNP	Senior researcher	0.1
24		Vladimir Malyshev	DLNP	Researcher	0.6
25		Nikolay Atanov	DLNP	Researcher	0.7
26		Ilia Zimin	DLNP	Researcher	0.7
27		Elena Plotnikova	DLNP	Researcher	0.5
28		Pavel Tsireshka	DLNP	Researcher	0.5
29		Vladimir Baranov	DLNP	Researcher	0.7
30		Ilya Vasilyev	DLNP	Researcher	0.7
31		Dmitry Dedovich	DLNP	Researcher	0.4
32		Viktoriya Moskalenko	DLNP	Junior researcher	0.7
33		Aleksandr Boikov	DLNP	Junior researcher	0.5
34		Viktoria Kiseeva	DLNP	Junior researcher	0.6
35		Oksana Dolovova	DLNP	Junior researcher	0.5
36		Anastasiya Tropina	DLNP	Junior researcher	0.6
37		Tatiana Lyubushkina	DLNP	Junior researcher	0.3
38		Alexey Kampf	DLNP	Junior researcher	0.8

39		Andrej Arbuzov	BLTP	Head of sector Deputy project leader	0.4
40		Serge Bondarenko	BLTP	Head of sector	0.3
41		Vladimir Zykunov	BLTP	Leading researcher	0.1
42		Maria Savina	BLTP	Senior researcher	0.1
43		Vladimir Bytev	BLTP	Senior researcher	0.5
44		Uliana Voznaya	BLTP	Trainee researcher	0.3
45		Vladimir Karzhavin	VBLHEP	Head of department	0.1
46		Valery Chmill	VBLHEP	Leading researcher	0.4
47		Faig Ahmadov	VBLHEP	Senior researcher	0.4
48		Alexander Lanyov	VBLHEP	Senior researcher	0.1
49		Vyatcheslav Shalaev	VBLHEP	Senior researcher	0.1
50		Viktor Pereygin	VBLHEP	Senior researcher	0.1
51		Ilya Zhizhin	VBLHEP	Researcher	0.1
52		Sergey Shmatov	MLIT	Director	0.1
53		Nikolay Voytishin	MLIT	Deputy director	0.1
54		Alexander Nikitenko	MLIT	Leading researcher	0.1
55		Olga Kodolova	MLIT	Leading researcher	0.1
56		Danila Oleynik	MLIT	Senior researcher	0.1
57		Artem Petrosyan	MLIT	Senior researcher	0.1
58		Igor Pelevanyuk	MLIT	Researcher	0.1
59		Kirill Slizhevsky	MLIT	Trainee researcher	0.1
60		Yury Korsakov	MLIT	Trainee researcher	0.1
61	engineers	Olga Atanova	DLNP	engineer	0.5
62		Vyacheslav Rogozin	DLNP	engineer	0.6
63		Andrey Shalyugin	DLNP	Senior engineer	0.4
64		Dmitry Budkovsky	VBLHEP	Engineer	0.1
65		Aleksandr Golunov	VBLHEP	Leading engineer	0.1
66		Yury Ershov	VBLHEP	Leading engineer	0.1
	specialists				

67	technicians	Alina Dadashova	DLNP	technician	0.3
68		Dmitry Kozlov	VBLHEP	technician	0.1
	<b>Total:</b>				<b>27.6</b>

### 3.2.2. JINR associated personnel (total number of participants)

№№ n/a	Category of employees	Partner organisation	Amount of FTE
1.	Scientific employees		0
2.	engineers		0
3.	professionals		0
4.	workers		0
<b>Total:</b>			<b>0</b>

## 4. Financial support

### 4.1. Total estimated cost of the project / subproject

Forecast of the total estimated cost (specify cumulatively for the whole period, excluding FPC).  
The details are given in a separate form.

600 kUSD

### 4.2. Extrabudgetary funding sources

Estimated funding from co-executors/customers - total.

Project Leader  / Davydov Yu.

Project Leader  / Zhemchugov A.

Date of submission of the project to DSOA: 20.05.2025

Date of decision of the laboratory's STC: 17.04.2025 document number: 2025-8

Year of the project opening: 2026

(for renewable projects) -- Project start year: 2025

**Schedule proposal and resources required  
for the implementation of the Project**

Names of costs, resources, sources of funding		Cost (thousands of dollars) resource requirements	Cost, distribution by year		
			1 <sup>st</sup> year	2 <sup>nd</sup> year	
	International cooperation (IC)	200	100	100	
	Materials	100	50	50	
	Equipment and third-party services (commissioning)	300	150	150	
	Commissioning work	-			
	Services of research organisations	-			
	Acquisition of software	-			
	Design/construction	-			
	Service costs ( <i>planned in case of direct project affiliation</i> )	-			
<b>Resources required</b>	<b>Normo-hours</b>	Resources			
		- the amount of FTE,	28.0	28.0	28.0
		- accelerator/installation,	200	100	100
		- reactor,....	600	300	300
<b>Sources of funding</b>	<b>Budgetary resources</b>	JINR budget ( <i>budget items</i> )	600	300	300
	<b>Extrabudgetary (supplementary estimates)</b>	Contributions by co-contractors			
		Funds under contracts with customers	0	0	0
		Other sources of funding			

Project Leader

 / Davydov Yu.

Project Leader

 / Zhomchugov A.

Laboratory Economist

 / Lisova

## ЛИСТ СОГЛАСОВАНИЙ ПРОЕКТА

НАИМЕНОВАНИЕ ПРОЕКТА: Разработка физической программы и детекторов для экспериментов на СЕРС

УСЛОВНОЕ ОБОЗНАЧЕНИЕ ПРОЕКТА: СЕРС

ШИФР ПРОЕКТА: 02-2-1151-1-2026/2027

ШИФР ТЕМЫ: 02-2-1151-1-2025/2027

ФИО РУКОВОДИТЕЛЕЙ ПРОЕКТА: Давыдов Ю.И., Жемчугов А.С.

СОГЛАСОВАНО:

ВИЦЕ-ДИРЕКТОР ИНСТИТУТА

ПОДПИСЬ

ФИО

ДАТА

ГЛАВНЫЙ УЧЕНЫЙ СЕКРЕТАРЬ  
ИНСТИТУТА

ПОДПИСЬ

ФИО

ДАТА

ГЛАВНЫЙ ИНЖЕНЕР

ПОДПИСЬ

ФИО

ДАТА

ДИРЕКТОР ЛАБОРАТОРИИ

ПОДПИСЬ

ФИО

ДАТА

ГЛАВНЫЙ ИНЖЕНЕР ЛАБОРАТОРИИ

ПОДПИСЬ

ФИО

ДАТА

УЧЕНЫЙ СЕКРЕТАРЬ ЛАБОРАТОРИИ

ПОДПИСЬ

ФИО

ДАТА

РУКОВОДИТЕЛЬ ТЕМЫ

ПОДПИСЬ

ФИО

ДАТА

РУКОВОДИТЕЛЬ ПРОЕКТА

ПОДПИСЬ

ФИО

ДАТА

РУКОВОДИТЕЛЬ ПРОЕКТА

ПОДПИСЬ

ФИО

ДАТА

ОДОБРЕН ПКК ПО НАПРАВЛЕНИЮ

ПОДПИСЬ

ФИО

ДАТА